Study of simultaneous variations of aerosol extinction on horizontal and slant radiation propagation paths

S.M. Sakerin, D.M. Kabanov, Yu.A. Pkhalagov, and V.N. Uzhegov

Institute of Atmospheric Optics,
Siberian Branch of the Russian Academy of Sciences, Tomsk

Received December 27, 2001

Statistical characteristics of aerosol extinction coefficients (ε_λ^A) and aerosol optical thickness (τ_λ^A) assessed from simultaneous measurements of atmospheric transparency in the wavelength range from 0.44 to 1.06 μm on horizontal and slant paths are considered. The height of the homogeneous atmosphere $H_0(\lambda) = \tau_\lambda^A / \varepsilon_\lambda^A$ is calculated from these data. It is shown that H_0 in the spectral range $\lambda = 0.44–0.56$ μm is about 1 km, and it decreases down to 0.6 km at $\lambda = 1.06$ μm. The correlation between ε_λ^A and τ_λ^A is analyzed. In general case the correlation between these parameters in summer is shown to be fairly weak with the value of 0.36–0.37 in the visible wavelength range at the significance level of 0.16. It is supposed that the correlation between these optical characteristics breaks due to practically independent dynamics of fine and coarse aerosol particles. To decrease the contribution of coarse aerosol to the variation of ε_λ^A and τ_λ^A, they were divided into the fine and coarse components. In this case the correlation between the fine components of ε_λ^A and τ_λ^A increases somewhat.

Introduction

In spite of the long history of research into aerosol extinction of radiation in the atmospheric surface layer ε_λ^A and in the atmospheric column $\tau_\lambda^A = \int \varepsilon_\lambda^A \, dh$, there are very few papers devoted to the problem of joint variations of these correlated characteristics (see, for example, Refs. 1–6). The aerosol extinction coefficients ε_λ^A were estimated from indirect data: either instrumental visual observations of meteorological range $S_m \approx 3.9/\varepsilon_{0.55}^A$ or nephelometric measurements of angular scattering coefficients. In the first case, the results have low accuracy and provide an idea about the effective extinction coefficient in the spectral range of human eye sensitivity. Nephelometric measurements (as a rule, at one angle and one wavelength) characterize, with acceptable accuracy, only the scattering coefficient caused by submicron aerosol.

The published results of investigations of two transparency characteristics are extremely contradictory: from the absolute absence of correlation[2] to the presence of strong correlation[4,5] at $S_m > 10–16$ km. The conclusions of Ref. 3 are likely the most realistic. This paper considered more than 400 events of joint measurements τ and S_m near Voeikovo (Leningrad Region) and showed that the correlation coefficient between them did not exceed 0.25–0.4. To be mentioned in this connection is Ref. 7, where the correlation between the scattering coefficients of dried aerosol at the altitudes from 0.3 to 3 km and the possibilities of parameterization of its vertical profile are analyzed. It indirectly follows from Ref. 7 that even in this case (only for the submicron component of dry aerosol) one can expect significant correlation based on classification of data according to atmospheric conditions: seasons, synoptic conditions, time of day.

Let us mention the possible reasons for correlation breaking between two transparency characteristics. The mechanisms of convection, turbulence, and transformation of aerosol properties (under the effect of humidity and insolation), as well as the processes related to cloudiness and alternation of pressure fields, can play a significant role in aerosol extinction in the atmospheric surface layer and in the atmospheric column. One of the consequences is the different response to the diurnal dynamics of atmospheric conditions right up to the contrary diurnal behavior of τ_λ^A and ε_λ^A (Ref. 1).

Reference 8 is the only one paper devoted to joint investigations of the spectral dependence of ε_λ^A and τ_λ^A. Variations and correlation statistics is not presented there, but the relative value of $H_0(\lambda) = \tau_\lambda^A / \varepsilon_\lambda^A$, which can be defined as an effective height or the height of the homogeneous aerosol layer, is analyzed. The variability range of H_0 from 0.44 to 1 km and its decrease with the wavelength increase are demonstrated with some examples.

In our opinion, the investigations of the joint variations of the spectral characteristics τ_λ^A and ε_λ^A are interesting and important because of two reasons. First, the use of the meteorological range S_m or other optical characteristic as an input parameter characterizing the

0235-6880/02/004 285-07 $02.00

aerosol optical thickness in radiation calculations requires more careful justification for different types of the optical weather and spectral ranges. Second, the analysis of the results of joint experiments will help us to better understand the processes of spatiotemporal transformation of different aerosol fractions.

At the first stage of our study, we consider the available results of independent experiments to analyze the most general properties and peculiarities of ε_λ^A and τ_λ^A variations in different wavelength ranges. This allows us to determine methods to be used and problems to be solved in further experiments.

1. Experimental conditions

The results of independent measurements of horizontal and slant atmospheric transparency near Tomsk in warm seasons of 1995–2000 were used for estimation of ε_λ^A and τ_λ^A variations and correlation. The join array $\{\varepsilon_\lambda^A, \tau_\lambda^A\}$ was formed from the series of observations of the aerosol optical thickness (AOT) of the atmosphere (hourly mean data). Then the corresponding values of ε_λ^A were calculated through interpolation for the time of τ_λ^A measurements. One can get the general idea about the number of data collected in different periods of measurements and about the atmospheric conditions from Table 1. The meteorological range S_m in the period of observations was relatively long and varying from 13 to 100 km.

Let us characterize briefly the instruments and methods used for determination of AOT and aerosol extinction coefficients in the atmospheric surface layer (Table 2). The spectral transparency of the atmospheric column was measured with a multiwave sun photometer[9] installed on a building roof at the height of ~ 18 m above the surface. Observations were carried out in short ~ 5 to 30 min series, when the sun was free of clouds. Then the hourly mean values were calculated from the obtained data. The techniques for photometer calibration and AOT determination with the use of LOWTRAN–7 software (Ref. 10) are generalized in Ref. 11. The atmospheric columnar water vapor W was measured with the sun photometer simultaneously with the aerosol component. So the data on joint water vapor variations in the atmospheric surface layer and the atmospheric column were sometimes involved for comparison.

The horizontal transparency of the atmosphere was measured with an automatic photometer.[12] The horizontal path was at the height from 5 to 12 m above the surface. The total radiation extinction was determined from the obtained transparency signals, and then the aerosol extinction coefficients ε_λ^A were separated using the method of multiple regression.[13] The periodicity of measurement cycles was 4 h in 1995–1999 and 3 h in 2000. The calculated values of ε_λ^A were then interpolated for comparison with AOT.

The diurnal behavior of the characteristics under study is exemplified in Fig. 1.

Table 1. The number of data $N\{\varepsilon_\lambda^A, \tau_\lambda^A\}$ and variations of meteorological parameters

Period	$N\{\tau_\lambda^A; \varepsilon_\lambda^A\}$	T, °C	a, g/m^3	RH, %
June 12–July 15, 1995	62	10.1–29.7	5.9–10.0	46.5–99.9
Aug 18–Sep 12, 1997	14	7.7–21.9	3.7–7.7	48–80
June 22–June 28, 1999	40	13.1–24.4	4.5–7.1	37–78.5
July 01–July 17, 2000	28	12.7–25.5	4.6–7.8	35.7–85.3
1995–2000	144	7.7–29.7	3.7–10.0	35.7–99.9

Table 2. Main characteristics of atmospheric transparency meters

Sun photometer	
Pass bands of interference filters*, μm	0.44, 0.48, 0.52, 0.55, 0.69 (0.67), 0.87, 1.06
Field of view, deg	0.75
Number of readings in hourly mean values	10–40
Error in τ_λ^A	0.01
Photometer of horizontal transparency	
Pass bands of interference filters*, μm	0.44, 0.48, 0.52, 0.55, 0.69, 0.84 (0.87), 1.06
Measurement path length, m	830
Number of readings in hourly mean values	6
Error in ε_λ^A, km^{-1}	0.01

* λ_{max} are given only for the compared wavelength ranges of the two instruments. Since filters were replaced in some years, the corresponding λ_{max} are given in parentheses.

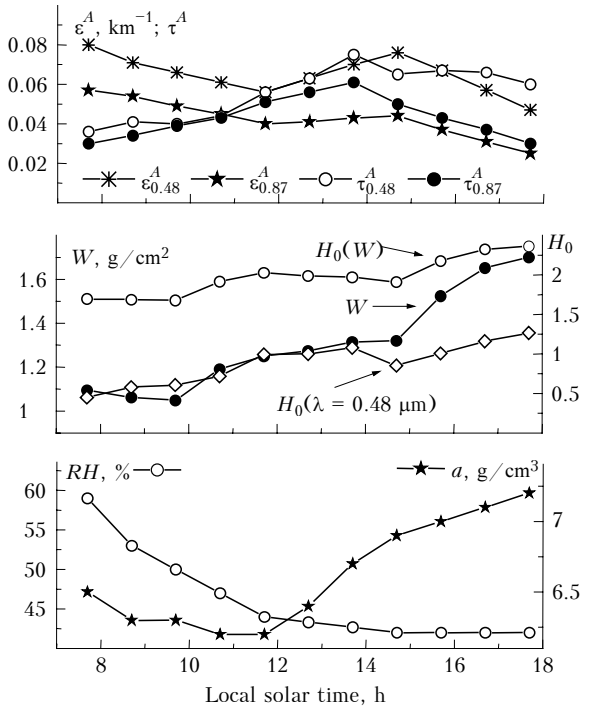

Fig. 1. Example of joint variations of optical and meteorological characteristics.

It is seen from Fig. 1 that the tendencies of τ^A_λ and ε^A_λ variations are different in different time: although weak, but contrary behavior before noon, and qualitatively the same dependence in the afternoon with the maximum turbidity at about 2 p.m. The diurnal dynamics of the effective heights of aerosol and water vapor was the same – permanent increase of the height during a day.

2. Peculiarities of spectral dependence of ε^A_λ, τ^A_λ, and the height H_0

The joint data array was statistically processed to reveal peculiarities in variation of ε^A_λ and τ^A_λ. The results are given in Table 3 and Fig. 2. It is seen that all statistical characteristics have the same spectral behavior, namely, the monotonic decrease with the increasing wavelength. The spectral dependence can be seen even in the variation coefficients V that characterize the relative variability. Nevertheless, the character of the spectral structure of ε^A_λ and τ^A_λ is different (Fig. 2*a*). In particular, the spectral dependence of τ^A_λ has more steep behavior starting from the central visible range and significantly less absolute values in the IR region as compared with ε^A_λ. The degree of selectivity estimated with the Angström parameter

$$\tau^A(\lambda) = \beta\lambda^{-\alpha}, \qquad (1)$$

is roughly twice as high as for AOT (Table 3). From the greater selectivity of τ^A_λ and less values in the IR region, it follows that the spectral differences are caused, first of all, by higher content of coarse aerosol in the atmospheric surface layer. (In principle, this result is expected, and the problem is in specific quantitative characteristics of the relative contribution of different-size particles).

Table 3. Statistics of τ^A_λ, ε^A_λ, and H_0 ($V = \sigma_X/\overline{X}$ are variation coefficients), α_τ and α_ε are the Angström parameters

Parameter	λ, μm	$\overline{X}$	σ_X	V	Min	Max
τ^A_λ	0.44	0.12	0.05	0.40	0.04	0.31
	0.48	0.11	0.04	0.40	0.03	0.29
	0.52	0.10	0.04	0.40	0.03	0.26
	0.56	0.09	0.04	0.41	0.03	0.23
	0.69	0.07	0.02	0.36	0.03	0.15
	0.87	0.05	0.02	0.36	0.02	0.12
	1.06	0.04	0.01	0.34	0.01	0.09
α_τ		1.23	0.51	0.42	0.01	2.54
ε^A_λ, km^{-1}	0.44	0.13	0.06	0.45	0.04	0.39
	0.48	0.12	0.05	0.43	0.04	0.36
	0.52	0.11	0.05	0.44	0.03	0.34
	0.56	0.11	0.05	0.43	0.02	0.29
	0.69	0.10	0.04	0.43	0.02	0.26
	0.87	0.09	0.04	0.42	0.01	0.19
	1.06	0.08	0.03	0.39	0.02	0.17
α_ε		0.54	0.30	0.56	0.07	1.83
H_0, km	0.44	1.02	0.51	0.50	0.22	3.77
	0.48	0.98	0.46	0.46	0.22	2.67
	0.52	1.03	0.52	0.50	0.22	3.29
	0.56	1.01	0.67	0.68	0.22	5.95
	0.69	0.80	0.52	0.66	0.18	3.63
	0.87	0.74	0.58	0.79	0.18	4.57
	1.06	0.61	0.40	0.65	0.12	3.19

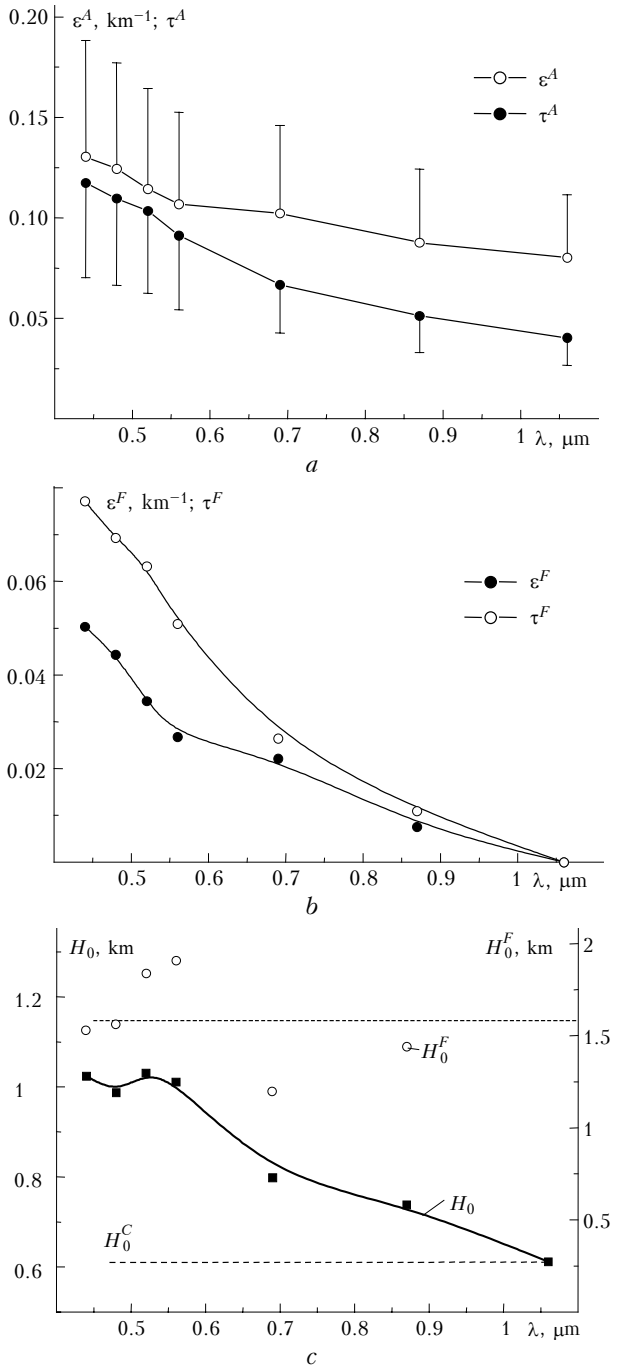

Fig. 2. Spectral behavior of mean values of aerosol extinction (*a*), fine components (*b*), and effective height H_0 (*c*).

When interpreting the data, we divided aerosol into only two fractions, namely, fine and coarse particles (according to their relative size $x = 2\pi r/\lambda$):

a) the relative size of fine particles lies in the range under the first maximum of the extinction efficiency factor, and this leads to the power dependence of the extinction on λ;

b) coarse particles of the size x in the range larger than the first maximum determine the quasi-neutral spectral dependence of aerosol extinction.

We can estimate the optical contributions of fine and coarse aerosol by representing the extinction characteristics in the form of two components, for example, for the coefficient ε_λ^A we have

$$\varepsilon_\lambda^A = \varepsilon^F(\lambda) + \varepsilon^C \approx \varepsilon_\lambda^F + \varepsilon_{1.06}^A, \qquad (2)$$

where the superscript F denotes the selective component of fine particles, and C denotes the contribution of the coarse fraction. It is seen from Fig. 2*b* that the spectral dependences of ε_λ^F and τ_λ^F also have different selectivity, likely because of different characteristics of the fine fraction in the atmospheric surface layer and in the entire column. However, it is early to draw some conclusions without inversion of the optical data and the estimate character of division (2).

The spectral peculiarities of ε_λ^A and τ_λ^A manifest themselves in the behavior of the effective height H_0 which gives an idea about the vertical profile of aerosol extinction. The height $H_0 \approx 1$ km in the visible wavelength region remains at the same level (see Table 3 and Fig. 2*c*) and then quickly decreases as the wavelength increases. The large variance of the effective height can raise some doubts in the reliability of the spectral dependence. Calculations performed according to the Student criterion have shown that the differences in H_0 in the range from 0.44 to 0.56 μm are not significant, and the difference with the range of 1.06 μm is significant with the confidence probability of 0.997. The decrease of the effective height in the IR region is a rather expectable result, because the coarse aerosol is largely concentrated in the atmospheric surface layer. Fine particles are more easily driven by wind and stored in the atmosphere, so the mean value of H_0^F is about 1.6 km. The presence of the spectral behavior of $H_0(\lambda)$ reflects re-distribution of the roles of the two fractions in different wavelength ranges. It should be also noted that the relative variability of H_0 increases in the IR region, and this evidences significant variations of the content of coarse aerosol just near the surface.

For comparison, let us present the values of the effective height H_0 obtained by other authors for the central visible range: 0.7 to 2, ~ 1.3, and 0.5 to 1 km, respectively, in Refs. 4, 5, and 8. The vertical distributions of molecular scattering and water vapor content are more homogeneous as compared with that of aerosol, and their effective heights are 8 km and about 2 km (in summer[14]), respectively. The mean height H_0 for the data array under consideration is 1.9 km.

3. Correlation and eigenvectors

The degree of correlation of the aerosol extinction characteristics at different wavelengths can be estimated by the correlation coefficients $\rho_\varepsilon(0.44; \lambda_i)$ and $\rho_\tau(0.44; \lambda_i)$ given in Table 4. (The critical value of correlation for the considered data array is 0.16 with the confidence probability of 0.95.)

Table 4. Correlation coefficients of aerosol extinction characteristics

λ, μm	0.44	0.48	0.52	0.56	0.69	0.87	1.06
$\rho_\varepsilon(0.44; \lambda_i)$	1	0.99	0.99	0.96	0.91	0.85	0.83
$\rho_\tau(0.44; \lambda_i)$	1	0.99	0.99	0.99	0.91	0.73	0.42
$\rho(\tau, \varepsilon)$	0.37	0.36	0.33	0.26	0.15	0.01	−0.04

As to spectral peculiarities, it should be noted that the near-surface coefficients ε_λ^A keep higher correlation values as the wavelength increases. The most possible reason is likely the same, namely, different contribution of coarse particles to aerosol turbidity in the atmospheric surface layer and the atmospheric column. For example, the contribution of the coarse fraction in the range 0.44 μm in the atmospheric surface layer is 61%, and that in the atmospheric column is only 30%. So the variations of τ^C are poorly seen in τ_λ^A in the shortwave range. It should be also noted that low values of AOT in the range of 1.06 μm approach the error value ($\Delta\tau \sim 0.01$–0.015). Consequently, the noise component that is not related to aerosol becomes apparent in the variance of $\tau_{1.06}^A$ variations.

Quite different situation is observed in the atmospheric surface layer. The significant contribution of ε^C keeps in the entire range, and variations of coarse aerosol provide for the coordinated change of ε_λ^A. Thus, we can conclude that the correlation $\rho_\tau(0.44; \lambda_i)$ is mainly related to fine particles and, together with τ_λ^F, it quickly decreases as the wavelength increases. The higher correlation $\rho_\varepsilon(0.44; \lambda_i)$ is largely supported by coarse aerosol.

As to the statistical correlation of AOT and the extinction coefficients, it can be noted that the significant correlation is observed only in the range up to 0.56 μm (see the lower row of Table 4). The practically independent dynamics of fine and coarse aerosol (especially, in different atmospheric layers) and their different optical contribution to formation of τ_λ^A and ε_λ^A lead to weakening and even break of correlation between the optical characteristics (Figs. 3*a* and *b*). Even selection of only fine components of ε_λ^F and τ_λ^F insignificantly increases their correlation (Fig. 3*c*).

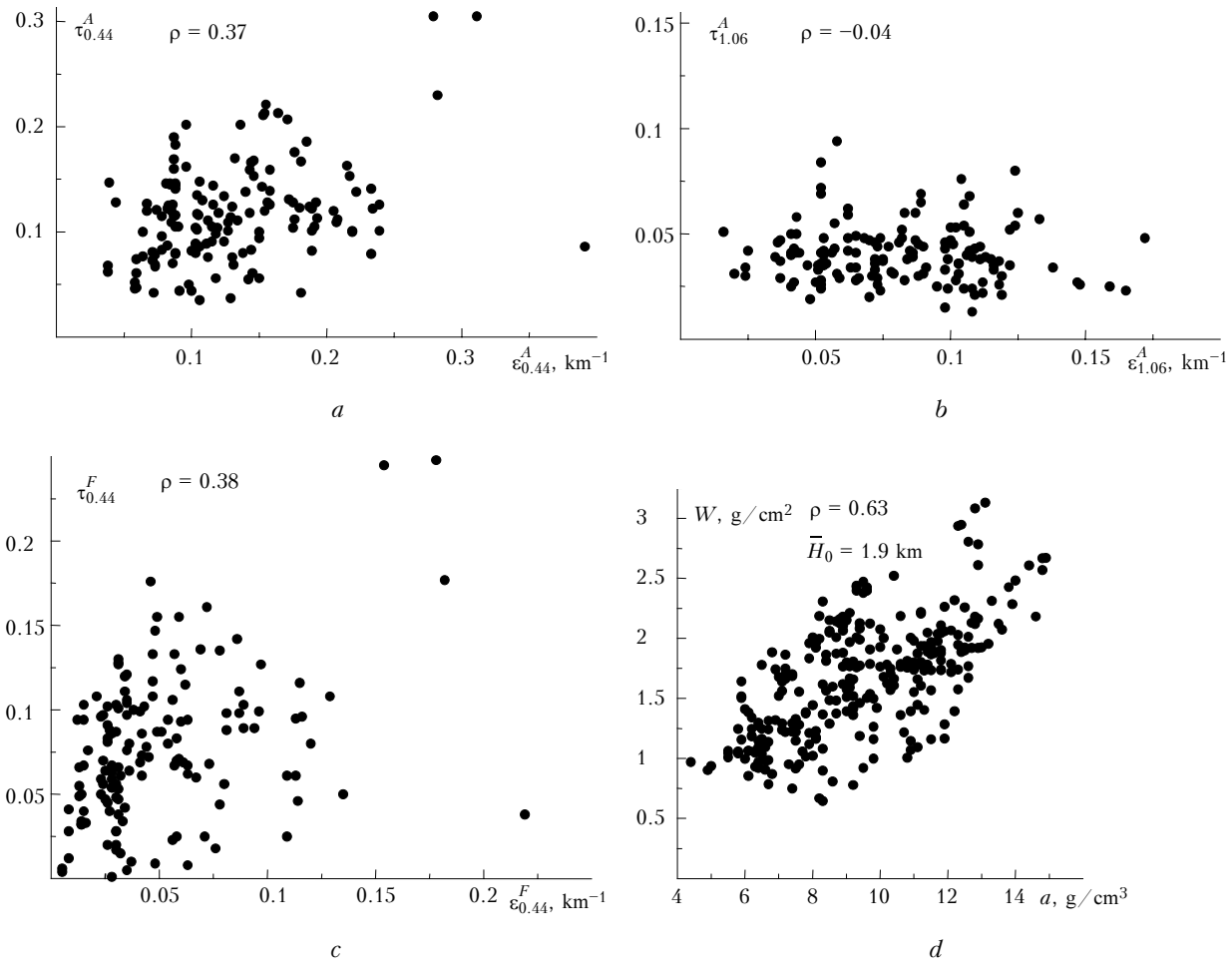

Fig. 3. Scatter diagrams of different components of aerosol extinction and humidity.

It is also necessary to note possible methodical reasons for poor correlation of near-surface and columnar extinction. Obviously, the content and variations of coarse aerosol are more significant near the surface. So, because of the different height of transparency meters (~ 8 and 18 m), the portion of aerosol recorded in the atmospheric surface layer does not reach the level of the sun photometer. The influence of the difference in the measurement paths should be referred, to some extent, to the submicron aerosol as well. Besides, a slight increase of the correlation when passing to the fine components $\{\varepsilon_\lambda^F, \tau_\lambda^F\}$ is related to the rough division of aerosol extinction into two components (2) on the assumption that $\tau^C = \tau^A_{1.06}$ (it would be more correct to use the values in the range of 2–4 μm, but we had no such data).

The correlation of the humidity characteristics is shown in Fig. 3*d* for comparison. In spite of the difference of processes related to humidity in the atmospheric surface layer and in the atmospheric column (for example, outflow of water vapor into cloudiness), the correlation remains quite high (0.63). As a consequence, the effective height of water vapor is more stable and slightly changes within one season.

The autocorrelation matrices $\rho_{\varepsilon(\lambda)\varepsilon(\lambda_k)}$, $\rho_{\tau(\lambda)\tau(\lambda_k)}$, and $\rho_{H_0(\lambda)H_0(\lambda_k)}$ allow calculation of eigenvectors $\varphi(\lambda)$ and eigenvalues (μ) of these matrices,[15] whose analysis formally enables us to estimate the number of factors forming the spectral structure of the parameters τ_λ^A, ε_λ^A, and H_0. The spectral behavior of two first eigenvectors $\varphi_1(\lambda)$ and $\varphi_2(\lambda)$ of the autocorrelation matrices $\rho_{\varepsilon(\lambda)\varepsilon(\lambda_k)}$, $\rho_{\tau(\lambda)\tau(\lambda_k)}$, and $\rho_{H_0(\lambda)H_0(\lambda_k)}$ is shown in Fig. 4 (curves *1–3*, respectively), and the eigenvalues μ_1 and μ_2 characterizing the portion of variance related to these vectors are given in Table 5.

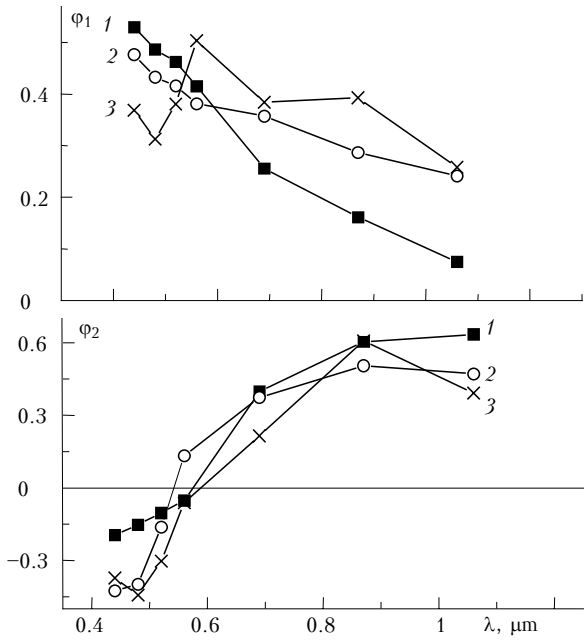

Fig. 4. Spectral behavior of two first eigenvectors of autocorrelation matrices of τ_λ^A (*1*), ε_λ^A (*2*), and H_0 (*3*).

Table 5. Eigenvalues of autocorrelation matrices

Parameter	Eigenvalue	
	μ_1	μ_2
τ_λ^A	0.948	0.040
ε_λ^A	0.949	0.044
H_0	0.885	0.077

Analysis of Fig. 4 and Table 5 enables us to note the following:

The spectrum of the vector $\varphi_1(\lambda)$ for τ_λ^A (curve *1*) differs from that of ε_λ^A (curve *2*) both in the character of the spectral behavior and in the absolute value. This confirms the above conclusion about the dominant role of fine aerosol in the variability of τ_λ^A and essentially smaller relative contribution of these particles to variations of ε_λ^A.

The spectrum of the vector $\varphi_1(\lambda)$ of H_0 has a pronounced minimum at $\lambda = 0.48$ μm and maxima at $\lambda = 0.56$ and 0.87 μm. It is difficult now to unambiguously interpret the non-monotonic structure of $\varphi_1(\lambda)$. Additional investigations are needed.

Almost 95% of τ_λ^A and ε_λ^A variance falls on the first eigenvector, which represents the contribution of spectrally constant-sign variations of these values, and 4% fall on the second eigenvector representing the contribution of alternating-sign variations.

As to the vector $\varphi_1(\lambda)$ of H_0, only 88% of variance falls on it in the considered data array, and 8% fall on the second vector.

Conclusion

The analysis has shown that in summer under conditions of relatively high atmospheric transparency ($S_m > 13$ km) the correlation of the characteristics of aerosol extinction in the atmospheric surface layer and in the atmospheric column is weak and significant only in the visible wavelength region. The reason for poor correlation is different optical contributions of fine and coarse aerosol to τ_λ^A and ε_λ^A, whose dynamics are practically independent and have singularities at different heights. The difference in optical influence of the two fractions on τ_λ^A and ε_λ^A manifests itself in the different selectivity of their spectral behavior ($\alpha_\tau = 1.23$ and $\alpha_\varepsilon = 0.54$) and significant decrease of the effective height H_0 (from 1 to 0.6 km) at the increasing wavelength. Actually, the dependence $H_0(\lambda)$ reflects re-distribution of the contributions of the two fractions, each having essentially different effective height $H_0^F \sim 1.6$ km and $H_0^C \sim 0.6$ km.

To be noted is the role of coarse aerosol, which makes the principal contribution (in the mean value and the variance) in the atmospheric surface layer, but is not so significant in the atmospheric column. So the success in modeling the correlation between τ_λ^A and ε_λ^A depends, first of all, on the possibility of parameterization of the coarse component of extinction (especially since the

possibility of realization of the similar problem for submicron aerosol has already been demonstrated[7].

The results obtained enable us to select the problems to be solved and the methods to be used for further research. First, to restrict the variety of external conditions, it is worth considering the joint variability of τ_λ^A and ε_λ^A in individual seasons and synoptic situations. Second, individual analysis of the diurnal dynamics of fine and coarse components of τ_λ^A and ε_λ^A (because of the different response to external conditions) and determination of the most significant meteorological predictors will be needed in the further studies. In this connection, the necessity of inverting the optical data $\{\tau_\lambda^A, \varepsilon_\lambda^A\}$ becomes more obvious, since it will allow more detailed analysis of peculiarities in the processes of aerosol transformation in the atmospheric surface layer and the atmospheric column.

Acknowledgments

The authors would like to thank R.F. Rakhimov for useful discussion of this paper.

This work was supported in part by the Russian Foundation for Basic Research (Grant No. 01–05–65197).

References

1. O.D. Barteneva, E.N. Dovgyallo, and E.A. Polyakova, Trudy Gl. Geofiz. Obs., Issue 220, 5–19 (1967).
2. O.D. Barteneva, N.I. Nikitinskaya, G.G. Sakunov, and L.K. Veselova, *Transparency of Atmospheric Column in Visible and Near-IR Spectral Regions* (Gidrometeoizdat, Leningrad, 1991), 224 pp.
3. V.P. Busygin, L.R. Dmitrieva, and N.A. Evstratov, Trudy Gl. Geofiz. Obs., Issue 448, 64–69 (1981).
4. Y.J. Kaufman and R.S. Fraser, J. Clim. and Appl. Meteorol. **22**, No. 10, 1694–1706 (1983).
5. T.C. Uboegbulam and J.A. Davies. J. Clim. and Appl. Meteorol. **22**, No. 8, 1384–1392 (1983).
6. J.T. Peterson, E.C. Flowers, G.J. Berri, C.L. Reynolds, and J.H. Rudisill, J. Appl. Meteorol. **20**, No. 3, 229–241 (1981).
7. M.V. Panchenko and S.A. Terpugova, Atmos. Oceanic Opt. **12**, No. 12, 1041–1045 (1999).
8. V.V. Lukshin, G.I. Gorchakov, and A.S. Smirnov, in: *Results of ODAEX–87 Comprehensive Aerosol Experiment* (Publishing House of the Tomsk Scientific Center SB AS USSR, Tomsk, 1989), pp. 70–76.
9. D.M. Kabanov, S.M. Sakerin, and S.A. Turchinovich, in: *Regional Monitoring of Siberia* (Spektr, Tomsk, 1997), Part 2, pp. 131–145.
10. F.X. Kneizys, E.P. Shettle, L.W. Abreu, J.H. Chetwynd, J.P. Anderson, W.O. Gallery, J.E.A. Selby, and S.A. Clough, *Users Guide to LOWTRAN-7*. AFGL-TR-0177 (1988), 137 pp.
11. S.M. Sakerin and D.M. Kabanov, J. Atmos. Sci. **59**, No. 3, 484–500 (2002).
12. Yu.A. Pkhalagov, V.N. Uzhegov, and N.N. Shchelkanov, Atmos. Oceanic Opt. **5**, No. 6, 423–426 (1992).
13. Yu.A. Pkhalagov and V.N. Uzhegov, Opt. Atm. **1**, No. 10, 3–11 (1988).
14. D.M. Kabanov and S.M. Sakerin, Atmos. Oceanic Opt. **10**, No. 1, 53–59 (1997).
15. A.M. Obukhov, Izv. Akad. Nauk SSSR, Ser. Geofiz. **1**, No. 3, 432–439 (1960).